Materials Science-Poland, *Vol. 28*, *No. 2*, *2010*

The effect of plasma torch power on the microstructure and phase composition of alumina coatings

L. MARCINAUSKAS[1, 2*], P. VALATKEVIČIUS[2]

[1]Physics Department, Kaunas University of Technology,
Studentu 50, LT-51368, Kaunas, Lithuania

[2]Lithuanian Energy Institute, Breslaujos 3, LT-4440, Kaunas, Lithuania

Alumina coatings were obtained by the atmospheric plasma spraying using Al_2O_3 nanopowders. The powders were injected into the anode zone of the torch. The microstructures and phase compositions of the coatings were determined by the scanning electron microscopy and X-ray diffraction. The results indicated that the higher the plasma torch power, the lower the surface roughness is. The as-sprayed coatings are composed of γ-Al_2O_3 and α-Al_2O_3, while the original powders were composed of δ-Al_2O_3 and γ-Al_2O_3 phases. The amount of γ-Al_2O_3 in the coatings increases from 56.52% to 100% if the plasma torch power is increased from 3.2 kW to 4.5 kW

Keywords: *Al_2O_3; plasma sprayed coating; plasma torch*

1. Introduction

Aluminum oxide (Al_2O_3) films are widely used as insulating and wear resistant coatings [1–4] due to their high resistance to corrosion and erosion, their hardness, and dielectric strength. It is well known that alumina has stable (α) and metastable (γ, δ, η, θ, β) polymorphs. Corundum (α-Al_2O_3) is the most widely used and best known alumina. Metastable γ-Al_2O_3 is used as a catalyst in the formation of bulk and fine chemicals, and in hydrocarbon conversion for petroleum refining [5]. Atmospheric plasma spraying (APS) is the most versatile method of achieving Al_2O_3 coatings. APS technology is used, because the high plasma temperatures are high enough to melt refractory ceramic materials (Al_2O_3, TiO_2, ZrO_2) [6–11].

Over the past decade extensive research has been devoted to the synthesis of ceramic coatings from nanopowders. It was demonstrated that nanostructured thermal spray ceramic oxide coatings could have higher wear resistance, superior hardness,

*Corresponding author, e-mail: liutauras@mail.lei.lt

and lower porosity when compared with similar coatings deposited from conventional powders [12–19]. It is well known that the final properties of the deposited coatings depend on various process parameters. The melting point of a particle strongly depends on the injection place of powders [6]. Yugeswaran et al. [7] showed that the hardness, porosity, and adhesive strength of ceramic coatings are related to the power of the plasma torch. Gao [8] found that alumina coatings deposited at higher arc currents and voltages are correspondingly harder and denser. The particle size of the powders also affects the hardness, phase content, and porosity of Al_2O_3 coatings [4, 10, 15]. However, using nanosized powder to deposit the coatings creates new problems. The most important difficulty is injection of the nanoparticles into the plasma. The nanoparticles, due to their low mass, cannot be injected directly into the plasma. To solve this problem, the nanoparticles are agglomerated into micrometer size particles. It was demonstrated that the optimum size of these particles lies in the range 10–100 μm [12–16]. The second challenge is to select appropriate process parameters which will retain crystal grain size at the nanometer regime in sprayed coatings [12, 16].

This paper presents a study on the formation of Al_2O_3 coatings from nanopowders, using the APS technology. The effect of various plasma torch power on the surface microstructure and phase composition of the alumina coating was investigated.

2. Experimental

A direct current plasma torch was used to deposit Al_2O_3 coatings (Fig. 1) [20, 21]. It consisted of a copper cathode (1), a working gas injecting ring with two tangential

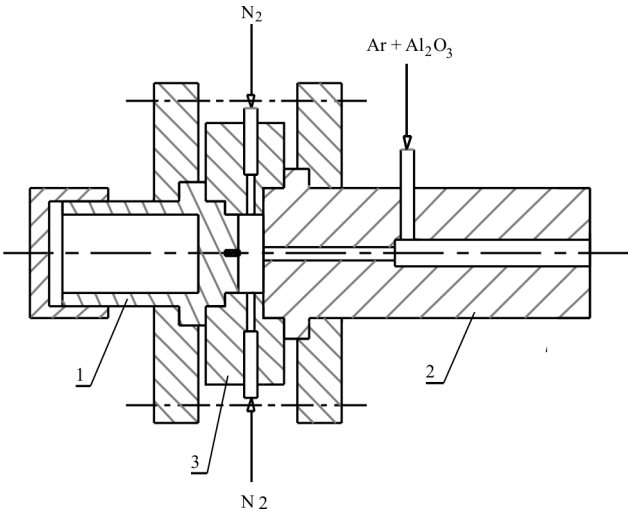

Fig. 1. Schematic diagram of the plasma torch:
1 – cathode, 2 – anode, 3 – gas injecting ring

blowholes (3), and an anode nozzle with a blowhole (2). Both electrodes were water cooled. The tangential injection of plasma forming gas stabilized the plasma. Nitrogen was used as the plasma forming gas (7.65 dm^3/min), while argon (1.20 dm^3/min) was used as the Al_2O_3 powder carrier gas. The powders were introduced through the anode nozzle, in order to improve the melting efficiency of the spray particles. The plasma torch was operated in an open atmosphere.

Ultra dispersion powder aluminium oxide (Sepros Corp. Int.), extracted by the gas dispersion synthesis method, was used as the starting material. The arithmetical mean of the Al_2O_3 nanoparticles was 87 nm, the apparent density – 3610 kg/m^3, the bulk density – 1890 kg/m^3, the melting temperature – 2320 K. The nanoparticles were composed of aluminum oxide (Al_2O_3) – 99.950%, magnesium oxide (MgO) – 0.011%, silicon oxide (SiO_2) – 0.007%, iron oxide (Fe_2O_3) – 0.002%, titanium oxide (TiO_2) – 0.001%, calcium oxide (CaO) – 0.017%, sodium oxide (Na_2O) – 0.009%. In order to make the nanosize oxide powders sprayable, the nanopowders were agglomerated into particles of 5–50 μm size and dried for 12 h at 473 K. The alumina ceramic coatings were sprayed on the stainless steel at various plasma torch powers. The deposition time for all coatings was 180 s. The detailed spray parameters are listed in Table 1.

Table 1. Deposition parameters and γ-Al_2O_3 phase fraction

Torch power [kW]	Spray distance [cm]	Mean plasma temperature (T_f) [K]	γ phase content (R) [%]
3.2	3.5	4665±20	56.52
3.75	3.5	5082±20	73.05
4.5	3.5	5603±20	100

In order to melt or partially melt the alumina, the temperature of the plasma should be higher than the melting point of Al_2O_3. According to the method presented in [20–22], it was found that the temperature of the nitrogen plasma at the exit of the anode nozzle may be estimated by the equation:

$$T_f = 36.8\left(\frac{I^2}{Gd_2}\right)^{0.225} \tag{1}$$

where I is the current (A), G – the nitrogen gas flow rate (kg/s), d_2 – the anode diameter (m), and T_f is the mean temperature of the plasma leaving the anode (K).

The surface morphology of the coatings was examined by the scanning electron microscopy (SEM), model JEOL JSM-5600. The coating structure was analyzed by X-ray diffraction (XRD) (DRON-UM1 with standard Bragg–Brentano focusing geometry) in a 10–70° range using CuK_α (λ = 0.154059 nm) radiation. Peak positions and full-width of peaks at half minimum intensity were obtained by fitting the data for the measured peaks with two Gaussian curves, in order to find the true peak position

and width corresponding to monochromatic $K\alpha_1$ radiation. The identification of phases was performed using the Crystallographica Search-Match program (Oxford Cryosystem Ltd, 1996-2003) for Powder Diffraction Data.

3. Results and discussion

3.1. Surface morphology

The agglomerated nanopowders observed with SEM are shown in Fig. 2a. The diameter of powder particles after agglomeration was 5–50 μm, and their shape was irregular.

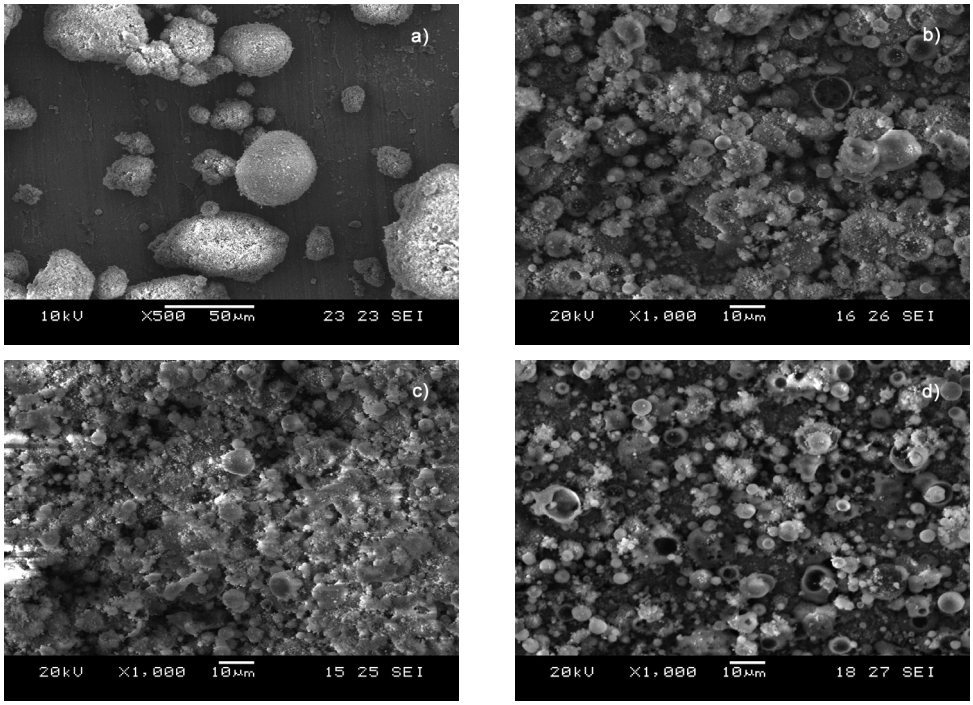

Fig. 2. SEM view of granulated aluminum oxide powders (a) and surface morphologies of the coatings deposited at various plasma torch powers: b) 3.2 kW, c) 3.75 kW, d) 4.5 kW

The surface morphologies of the as-sprayed Al_2O_3 coatings are presented in Fig. 2. The surface roughness decreases with the increase in the plasma torch power. The coatings consist mostly of splats and particles 0.5–10 μm wide. The surface of the coating deposited under 3.2 kW is composed of a relatively higher number of splats 5–10 μm wide. The coating produced at 3.75 kW mostly consists of ~5 μm splats (Fig. 2c). The coating obtained at the highest torch power beside discrete 5–10 μm

splats, have the highest number of splats and grains, whose size is lower than 1 μm (Fig. 2d). Beside the micrometer size splats, spherical nanosize (100–200 nm) particles were found on the surface of the coatings under larger magnification. It may be noted that all coatings have some pores, which is typical of the coatings produced by plasma spray.

The differences in the surface morphology depend on the input power. The feedstock granules were of various sizes (from 5 to 50 μm), and the momentum transferred from the plasma gas to the particles strongly depends on the mass of the injected granules. Large granules attain a lower velocity compared with the smaller ones. Usually, the larger particles tend to penetrate the core and travel around the periphery of the plasma jet, as a consequence of their larger inertia. Meanwhile, the smaller granules are near to the hottest core of the plasma jet [4]. Thus, the large total heat capacity will be higher for the larger size particles, and the larger particles need more time to be melted. The higher plasma torch power provides better heating and a higher melting degree of the particles. Eventually, the coatings will be composed of smaller size splats and particles, and the number of fully melted regions is also higher. Yugeswaran [7] indicated that the coatings deposited at higher plasma temperatures (input powers) exhibit a fine type structure, having lower surface roughness and fewer cracks formed in the solidification process. Song et al. [13] established that the coatings sprayed at higher heat input powers have a lower volume fraction of pores and fewer partially melted regions.

3.2. XRD characterization

The X-ray diffraction (XRD) patterns of the starting powders indicate that the powders are composed of two phases: δ-Al_2O_3 and γ-Al_2O_3 (Fig. 3). XRD studies revealed that dominant phases in the sprayed coatings are γ-Al_2O_3 and α-Al_2O_3 (Fig. 4). It may be noted that no δ-Al_2O_3 phase was obtained in the sprayed coatings. The coating deposited at the lowest power (3.2 kW) had peaks attributed to (113), (104), (012) alpha and (400), (440), (311) γ-Al_2O_3. The intensities of the γ-Al_2O_3 diffraction peaks increase with the increase in the plasma torch power (Fig. 4), whereas those of the α-Al_2O_3 peaks decrease. Thus the XRD patterns of the coating deposited at the highest power have the lowest intensity peaks, however only cubic γ-Al_2O_3 phase is obtained. These results indicate that the amount of γ-alumina increases and the amount of α-Al_2O_3 decreases as the power of the plasma torch increases.

The relative amount of the major phases was calculated from the XRD intensity data [23, 24]:

$$R = \frac{I_{(400)}^{\gamma\text{-}Al_2O_3}}{I_{(113)}^{\alpha\text{-}Al_2O_3} + I_{(400)}^{\gamma\text{-}Al_2O_3}} \times 100\% \tag{2}$$

where R is the γ-Al_2O_3 phase content, $I_{(hkl)}$ is the intensity of the peak diffraction for the corresponding plane of the α-Al_2O_3, and γ-Al_2O_3 phases.

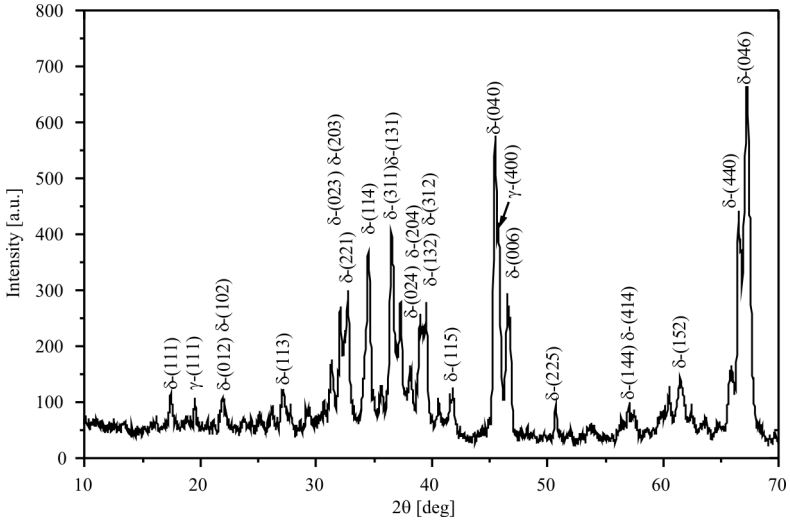

Fig. 3. X-ray diffraction patterns of the granulated Al_2O_3 nanopowders

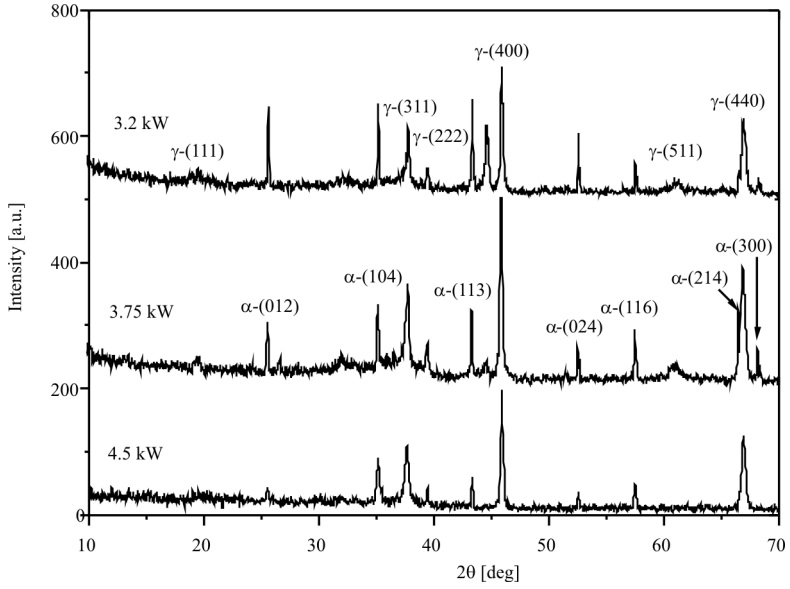

Fig. 4. XRD diffraction patterns of the sprayed Al_2O_3 coatings.

The results for phase compositions calculated from XRD data are presented in Table 1. The cubic γ-Al_2O_3 content was about 56.52%, at 3.2 kW. When the plasma torch power reached 3.75 kW, the γ-Al_2O_3 content increased to 73.05. The coating produced at 4.5 kW shows only peaks corresponding to γ-alumina phase. Gao et al. [8] also showed that the amount of γ-Al_2O_3 in the coatings increases and amount of α-Al_2O_3 decreases as the plasma power increases. Zeng [15] reported that the γ-Al_2O_3 content in the coatings will be higher when the particle size of the starting powder is smaller.

The residence time of Al_2O_3 powder inside the plasma jet is usually lower than 10^{-3} s. The melting points of the powders are higher for powders having smaller particle sizes. It is generally accepted that during solidification on impact, γ-Al_2O_3 is homogenously nucleated if the initial droplet is completely melted. Most authors [4, 7, 8, 15] suggest that the amount of γ-alumina in the coating represents the melting extent of the powders. The existence of α-Al_2O_3 in the sprayed coatings is attributed to both unmelted particles and to a solid-state γ-to-α phase transformation [25]. It is well known that the phase formation of the coatings is influenced by heat transferred from the plasma to the Al_2O_3 particles; the quenching rate of molten particles; the shape and size of the powder particles [4, 7]. The plasma flow temperature increases as the torch power increases (see Table 1). So, a higher fraction of the Al_2O_3 powder will melt, and consequently the coatings will consist of higher amounts of γ-Al_2O_3. The higher amount of gamma alumina produced is attributed to the high cooling rate ($\sim 10^6$ K/s) of the molten granules during spraying. Furthermore, according to the laws of nucleation kinetics, γ alumina is more easily nucleated from the melt state than α-Al_2O_3 because of the lower interfacial energy between the γ alumina structure and the liquid [26]. The experimental results indicated that the granulated powders are completely melted at 4.5 kW torch power.

4. Conclusions

Al_2O_3 coatings were successfully deposited by the APS technique using nanopowders. The surface morphology and phase composition of the coatings were studied. SEM results indicated that the coatings produced at higher plasma torch power are composed of smaller sized splats and particles. XRD measurements revealed that the as-sprayed coatings were composed from γ-Al_2O_3 and α-Al_2O_3. The increase in the plasma torch power increases the melting degree of the powders, and consequently the amount of γ-Al_2O_3 phase in the coatings will be higher. The coating deposited at 4.5 kW is composed exclusively from γ-Al_2O_3 phase.

References

[1] MASALSKI J., GLUSZEKA J., ZABRZESKI J., NITSCH K., CLUSZEK P., Thin Solid Films, 349 (1999), 186.
[2] YOUNG E.J., MATEEVA E., MOORE J.J., MISHRA B., LOCH M., Thin Solid Films, 377–378 (2000), 788.
[3] IRISAWA T., MATSUMOTO H., Thin Solid Films, 509 (2006), 141.
[4] YIN Z., TAO S., ZHOU, X., DING C., J. Eur. Ceram. Soc., 28 (2008), 1143.
[5] FU L., JOHNSON D.L., ZHENG J.G., DRAVID V.P., Amer. Ceram. Soc., 86 (2003), 1635.
[6] FAUCHAIS P., VARDELLE A., DENOIRJEAN A., Surf. Coat. Technol., 97 (1997), 66.
[7] YUGESWARAN S., SELVARAJAN V., SEO D., OGAWA K., Surf. Coat. Technol., 203 (2008), 129.
[8] GAO Y., XU X., YAN Z., XIN G., Surf. Coat. Technol., 154 (2002), 189.
[9] CTIBOR P., BOHAC P., STRANYANEK M., CTVRTLIK R., J. Eur. Ceram. Soc., 26 (2006), 3509.
[10] WESTERGARD R., ERICKSON A., AXEN L.C.N., HAWTHORNE H.M., HOGMARK S., Tribol. Int., 31 (1998), 271.

[11] BRINKIENE K., KEZELIS R., J. Eur. Ceram. Soc., 25 (2005), 2181.
[12] SHAW L., GOBERMAN D., REN R., GELL M., JIANG S., WANG Y., XIAO T.D., SRRUTT P.R., Surf. Coat. Technol., 130 (2000), 1.
[13] SONG E.U., AHN J., LEE S., KIM N.K., Surf. Coat. Technol., 201 (2006), 1309.
[14] LIMA R.S., MARPLE B.R., Surf. Coat. Technol., 200 (2006), 3428.
[15] ZENG Y., LEE S.W., DING C.X., Matter. Lett., 57 (2002), 495.
[16] GADOW R., KERN F., KILLINGER A., Mater. Sci. Eng. B, 148 (2008), 58.
[17] CHEN H., ZENG Y., DING C., J. Eur. Ceram. Soc., 23 (2003), 491.
[18] ZENG Y., LEE S., GAO L., DING C. X., J. Eur. Ceram. Soc., 22 (2002), 347.
[19] HUI R., WANG Z., KESLER O., ROSE L., JANKOVIC J., YICK S., MARIC R., GHOSH D., J. Pow. Sourc., 170 (2007), 308.
[20] AKDOGAN E., COKELILER D., MARCINAUSKAS L., VALATKEVIČIUS P., VALINČIUS V., MUTLU M., Surf. Coat. Technol., 201 (2006), 2540.
[21] MARCINAUSKAS L., VALINČIUS V., VALATKEVIČIUS P., GRIGONIS A., Power Engineering, 1 (2006), 36. (in Lithuanian).
[22] VALINČIUS V., KRUŠINSKAITE V., VALATKEVIČIUS P., VALINČIŪTE V., MARCINAUSKAS L., Plasma Sources Sci. Technol., 13 (2004), 199.
[23] CAO L.H., KHOR K.A., FU L., BOEY F., Mater. Process. Technol., 89-90 (1999), 392.
[24] KHOR K.A., BOEY F.Y.C., ZHAO X.L., CAO L.H., Mater. Sci. Eng., A300 (2001), 203.
[25] YILMAZ S., IPEK M., CELEBI G.F., BINDAL C., Vacuum, 77 (2005), 315.
[26] MCPHERSON R., Thin Solid Films, 83 (1981), 297.

Received 16 March 2009
Revised 20 September 2009